18th International Conference on Renewable Energies and Power Quality (ICREPQ'20)
Granada (Spain), 2nd to 4th September 2020
Renewable Energy and Power Quality Journal (RE&PQJ)
ISSN 2172-038 X, Volume No.18, June 2020

Bio-inspired aerofoils for small wind turbines

R. Mulligan

Institute of Mechanical, Process and Energy Engineering, School of Engineering and Physical Sciences,
Heriot-Watt University
Riccarton, Edinburgh EH14 4AS (Scotland, UK)
Phone/Fax number:+0049 131 451 4374 / 3129, e-mail: **rm96@hw.ac.uk**

Abstract. This paper investigates the effectiveness of modifying the design of wind turbine blades for small wind turbines. Taking inspiration from nature, the two modifications explored were spanwise corrugations of the blades inspired by a dragonfly's wing structure, and flexible blades inspired by the shape-morphing of birds and insect wings that adapt to the air conditions.

Two types of corrugations were tested in a wind tunnel with the results that the corrugated nature appeared to have desired effects on delaying stall by 4° and reduced the detriment of post-stall behaviour. In addition, the corrugated skin displayed similar characteristics to the control aerofoil, with a small reduction in the peak lift to drag ratio of 7.3%. In the second section, a rigid turbine blade was compared a semi-flexible and fully flexible blade by altering the Young's modulus using the QBlade simulation tool. Although, spanwise deflection was high in the flexible blade, a reduction in the peak stresses was shown.

Key words. Aerodynamics, aeroelasticity, biomimetics, boundary layer control, renewable energy

1. Introduction

While most research is focused on increasing the capacity of commercial wind farms, 1 in 10 people still lack access to electricity. They live predominantly in rural areas, where small off-grid wind turbine systems could be the best solution in tackling energy poverty.

Utility-scaled turbines have a highly optimised shape and operational control, matching rotor rotation rate and blade pitch to the current wind conditions. In contrast, small wind turbines usually have a much simpler turbine blade shape and little control, especially in cases where the turbines are built in regions where local construction facilities might be limited. In these conditions, many opportunities have arisen to optimise the energy production with new turbine blade designs to improve aerodynamic performance under a wide range of operating conditions with little active control. One option is to find a suitable blade surface shape for a rigid blade design, as explored in this paper in using a corrugated blade surface. Another option is to explore passive control with a flexible blade that has the potential of reducing the loading on the blade and/or the ability to change pitch to work at optimal conditions for each wind speed. Both options can be found in nature.

A. Biomimicry

Biomimicry is finding solutions to human design problems by taking inspiration from nature's strategies, developed from millions of years of evolution. Nature-inspired ideas already have prominent applications in the wind industry where a company called Wind Power uses leading edge modifications inspired by whale tubercles to increase energy output of wind turbines blades by delaying stall [1].

Fluid structure interaction models of plants with light weight and flexible characteristics allow them to tolerate high wind forces through energy dissipation to prevent structural failure [2]. Insects take advantage of wing flexing during flight, with a numerical study on beetle wings [3] highlighting the significance of a flexible wing in changing the twist angle and camber so that less thrust is required for the same amout on lift.

B. Small wind turbine challenges

While birds have evolved to morph their wing shapes to the flight and manoeuvre conditions, manufactured wings require control to achieve wing morphing. The use of morphing wings for wind turbines has been explored in principle [4], for horizontal-axis wind turbines [5] and vertical-axis wind turbines [6].

However, for small wind turbines, the added complexity and costs of adding active control to wind turbines is excessive both, compared to their current manufacturing costs and to their potential electricity yield. Viable options to improve the performance small turbine rotors will have to rely on turbine blade design and passive control. Turbine blade design can consider the spanwise shape or the aerofoil shape, while passive control might be achievable through passively morphing wings.

C. Flexible blades

Wind turbines tend to be subject to deflections due to aerodynamic loading during operations, and the use of flexible blades as a form of passive pitch control has been previously explored. Wind tunnel studies have shown that an elasto-flexible lifting surface increases the chamber thus increases lifting capabilities and postpones stall onset

[7], preventing the sudden drop in lift, and has been shown to increase the energy production of the wind turbine by up to 35% [8].

D. Aerofoil profile alterations

Research has looked at altering the entire shape of the aerofoil surface to alter the aerodynamic properties. A study by Manshadi [9] looked at the effect of a top jagged wall on the top surface of an aerofoil to reduce the shock wave interactions on the boundary layer to reduce overall wave drag and weaken shockwaves during transonic flight. The shock disintegration was most pronounced with triangular jagged shapes and enables an opening to explore dragonfly-inspired structures at high Reynolds numbers.

In studying the effects of skins which are corrugated on both sides, Xia [10] concluded that a corrugated skin can delay stall, where eddies form in the troughs which effectively smooth over the airflow like that of streamlined aerofoils. Increasing the size of corrugations caused a reduction in lift and an increase in drag so a corrugated skin must be optimally tuned.

E. Aims and objectives

This paper considers two bio-inspired methods for improving the performance of small wind turbines. First, the effect of surface corrugation on aerofoil performance was tested in a wind tunnel and secondly, passive control through a flexible blade structure was explored using the QBlade [11] open source platform.

2. Methodology

A. Design of aerofoils

The control aerofoil was a NACA 4416 aerofoil as shown in Figure 1(a) with its design details listed in table I. The span was the full length of the test chamber, effectively giving an infinite aspect ratio.

The second aerofoil, Figure 1(b), is inspired by the corrugated dragonfly wing vein structure (Aeshna cyanea) which has a deep groove corrugated structure, with the dimensions based on micro-CT images of a dragonfly wing cross section. Since the focus was on the top surface boundary layer, the corrugations were placed on the top only, and were slightly asymmetrical to mimic the natural shape of a dragonfly's wing. Based on previous studies, a change in shape of the top surface has demonstrated improved lift and drag characteristics.

Table I. – Details of the Control Aerofoil: NACA 4416

VARIABLE	VALUE	UNITS
Chord length, *c*	0.12	m
Span, *b*	0.45	m
Maximum thickness/chord ratio, *t/c*	16	%
Position of maximum thickness	40	%
Chamber	4	%
Zero lift angle	-4	°

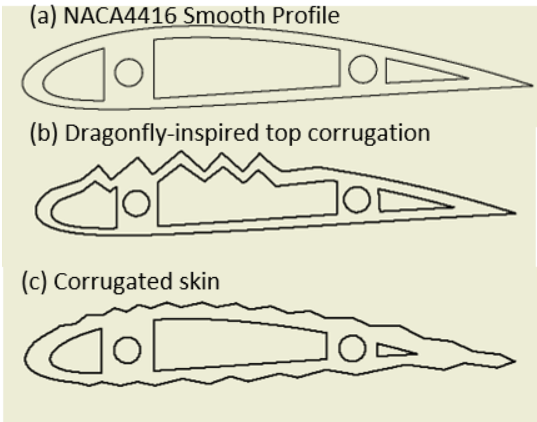

Fig.1. Aerofoil designs

The third aerofoil, Figure 1 (c), is based on research around corrugated skin on aerofoils to improve performance. The design of these grooves is shallower and contains the groove structure all over the aerofoil surface. The shallower grooves should create smaller vortices and cause less drag than the aggressive profile of the top corrugated aerofoil, while hoping for an improvement on the lift/drag ratio. The leading edge of all three designs was identical to keep the design variables limited.

The dragonfly inspired aerofoil in Fig. 1(b) will be here referred to as the '*top corrugated*' while the aerofoil in Fig. 1(c) will be referred to as the '*corrugated*' aerofoil.

B. Wind Tunnel tests

The three aerofoils described in §2.A were tested in a recirculating wind tunnel with a square test section of dimension 450 mm x 450 mm, with a design wind velocity of up to 12 m/s, which resulted in tests covering a range of Reynolds numbers from around 40 000 to 52 000. The wind speed was measured with an inclined manometer tube giving velocity readings with an accuracy of ±2.5%.

The aerofoil in the test chamber was held in place by a force gauge rig where the front and rear lift forces, $F_{L,f}$ and $F_{L,r}$, and the drag force, F_D, were measured. The reading accuracy of the load cells was better than ±0.1% but fluctuations in the readings resulted in a final uncertainty in the lift and drag forces comparable to the uncertainty in the wind speed. From the load cells, the drag, lift, and moment coefficients, C_D, C_L and C_m respectively, were calculated as

$$\boldsymbol{C_D = \frac{F_D}{\frac{1}{2}\rho b\, c\, U^2}} \quad (1)$$

$$\boldsymbol{C_L = \frac{F_{L,f} + F_{L,r}}{\frac{1}{2}\rho b\, c\, U^2}} \quad (2)$$

$$C_m = \frac{d_f F_{L,f} - d_r F_{L,r}}{\frac{1}{2}\rho b\, c\, U^2} \quad (3)$$

where $\rho = 1.225\ \mathrm{kg\ m^{-1}}$ is the density of air, and b the span and c the chord as given in Table I.

The lift and drag forces were measured for each aerofoil over a range of angles of attack from –4° to 40°, set manually with an uncertainty of –0.5° to + 1.5°

C. Blade Element and Structural modelling

To explore the effectiveness of flexible blades, a numerical approach had to be taken due to the national closure of laboratory facilities during the COVID-19 pandemic. For this, the QBlade simulation tool was used to modify an existing reference rotor by changing the material properties of the blades.

QBlade is a tool that implements Blade Element Momentum (BEM) theory [12] to obtain the performance parameters through solving the momentum balance of the wind turbine. The blade was divided into 20 sections as shown in Figure 3, and the lift and drag force are calculated locally at each section. BEM is based on the assumptions of two-dimensional effects only. Three-dimensional correction was applied with the Prandtl tip loss factor, root deflection correction, and a Reynolds number drag correction.

A turbulent wind field and wind shear is important to factor into simulations as small wind turbines are normally situated near buildings and villages. The integration of the FAST module created by the National Renewable Energy Laboratory (NREL) [13] performs aeroelastic simulations. It can solve for unsteady flow and structural dynamics to consider the effect of wind fluctuations.

It is used in the design and optimisation stage development of horizontal and vertical axis turbines. The advantage is the low computing power required vastly speeds up research and development of new concepts compared to the computer intensive CFD programmes. QBlade has been validated with other solvers and experiments, proving a high degree of accuracy and reliability.

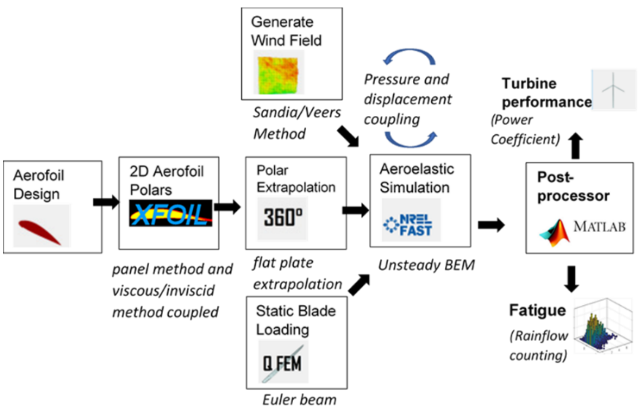

Fig. 2. Flow diagram of the QBlade features and methods with screenshots from the application [11]

The wind turbine was modelled based on the Aerogenesis 5 kW double-blade horizontal-axis turbine situated at the University of Newcastle, Australia with a rotor diameter of 5 m.

The aeroelastic properties of this turbine have been studied using the NREL FAST simulation tool and validated with experimental recordings. The turbine has yaw control using a passive tail fin and has a cut-in wind speed of 3.5 m/s, a rated wind speed of 10.5 m/s which equates to a rotor speed of 200 rpm at a tip speed ratio of 7. At the hub height of 18 m, the measured average wind speed was 7.5 m/s.

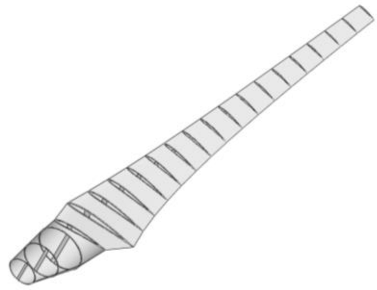

Fig. 3. Blade Design

The blade in Figure 3 of radius 2.5m was modelled on the NACA 4412 foil, using the in-built function to optimize the chord length and pitch angle of each segment. In order to study the effects of blade flexibility on the turbine performance, a coupled aeroelastic simulation was performed. It combined the aerofoil polar, structural properties and a generated wind field as shown in Figure 2 with a turbulence intensity of 18% and worked by transferring data of the pressure forces and node displacement between iterations in the FAST module. To obtain the results, the structural loads and turbine performance were then post-processed using MATLAB.

To compare the results of blade flexibility three blades of varying Young's moduli were modelled as represented in Table II.

Table II. – Blade Material Properties

MATERIAL	FLEXIBILTIY	YOUNG'S MODULUS (GPa)
Carbon Fibre	Rigid	73
E-glass/Epoxy	Semi-Flexible	40
Bamboo/Poplar	Fully Flexible	10

E. Fatigue Damage Using Rainflow-Counting

The lifespan of the turbine is determined by the damage caused by cyclic stress loading. The greatest stress occurs at the blade root, and the equivalent stress [14] on this area is calculating by combining the force and bending moments imported from the FAST simulation:

$$\sigma_{eq} = \frac{F_z}{A}\,\frac{\sqrt{M_x + M_y}}{W_b} \quad (4)$$

Where $\mathbf{F_z}$ is the Axial force (N), $\mathbf{M_x}$ and $\mathbf{M_y}$ are the edgewise and flapwise moments (N.m) respectively, $\mathbf{A}$ is the circular area of the blade root (m^2) and $\mathbf{W_b}$ is the modulus of the root section of the blade (m^3).

The continuous stress loading and unloading cycles can be counted and measured and then sorted depending on its amplitude and mean into a 3D histogram using the rainflow counting algorithm to determine the number of fatigue cycles. With enough successive damage cycles, the blade will break. According to Miners Rule [14], this occurs when the cumulative damage, D, reaches 1:

$$\boldsymbol{D} = \sum_{i} \frac{\boldsymbol{n_i}}{\boldsymbol{Ni}} \tag{5}$$

Where $\mathbf{n_i}$ is the number of load cycles for a given stress amplitude/mean combination obtained from the rainflow and $\mathbf{N_i}$ is the number of permissible load cycles to failure for a given stress amplitude/mean combination [14] calculated as follows:

$$\boldsymbol{Ni} = \left[\frac{\boldsymbol{X_t} + |\boldsymbol{X_c}| - |2\boldsymbol{\gamma_{Ma}\sigma_m} - \boldsymbol{X_t} + |\boldsymbol{X_c}||}{2\left(\boldsymbol{\gamma_{Mb}}/\boldsymbol{C_{1b}}\right)\boldsymbol{\sigma_a}}\right]^{\boldsymbol{m}} \tag{6}$$

Where

- $\mathbf{X_t}$: Tensile Strength (MPa)
- $\mathbf{X_c}$: Compressive Strength (MPa)
- $\boldsymbol{\sigma_m}$: Mean Stress (MPa)
- $\boldsymbol{\sigma_a}$: Stress Amplitude (MPa)
- $\boldsymbol{\gamma_{Ma}}, \boldsymbol{\gamma_{Mb}}, \boldsymbol{C_{1b}}$: Safety Factors
- $\mathbf{X_c}$: Compressive Strength (MPa)
- **m**: Slope of S-N curve

3. Results

The results are split into the two main work packages, first covering the wind tunnel results comparing rigid aerofoil shapes, while the second part presents results on the response of a flexible aerofoil and turbine rotor.

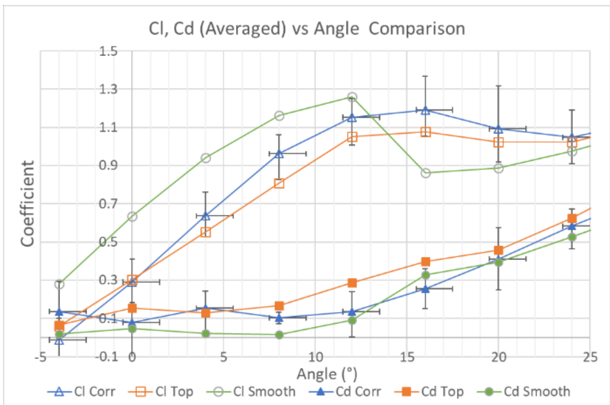

Fig. 4. Lift and drag coefficients versus angle of attack for corrugated, top corrugated and smooth aerofoils.

A. Effects of Corrugation on Performance

Figure 4 shows the lift and drag coefficients for the three test aerofoils against angle of attack. Comparing the lift, the smooth aerofoil gives the highest lift reaching its maximum around 12°, however, suffers from rapid loss of lift straight after separation due its smooth profile.

Both the corrugated and top corrugated shapes in Figure 4 show a significant improvement in delaying the stall by 4° and have a longer transition before complete boundary layer separation. Both managed to avoid the rapid loss of lift observed in the smooth profile. Dynamic stall can be problematic in wind turbine operation, where dynamic instability reduces the fatigue life of the turbine. Previous studies have discussed how the vortices provide a suction force on the boundary layer to keep it attached to the top surface of the aerofoil.

The corrugated aerofoil has a small reduction of 7.3% in the peak lift to drag ratio compared to the smooth aerofoil. Aerodynamic performance greatly reduces for the top corrugated aerofoil, with a peak lift to drag ratio reduction of 52.6% compared to the smooth aerofoil due to high drag caused by an early separation of the boundary layer.

The lift and drag results oppose the lift benefits shown by several studies, with both corrugated aerofoils displaying a reduction in lift. In previous studies where corrugation increased lift, the whole aerofoil displayed a corrugated shape and it is possible that a sharp leading edge provided vortex lift to give the aerofoils an increased lift advantage. Since the nose was kept rounded as a control for this study, these vortex lift benefits were not displayed. The lift and drag results varied with the size of corrugation suggesting that in future studies the corrugation shape can be optimally tuned.

This led to the suggestion that a morphing or flexible wing surface could be used to reach more desirable lift and drag forces than a rigid aerofoil. The first stage of this research is outlined in the following section.

B. Effects of Flexibility on Performance

The second set of work explored the response of a flexible turbine blade on rotor performance in QBlade. The normal and tangential forces recorded from the FAST simulation were imported into the FEM module where the displacement of the blade along the entire blade span in the flapwise direction (figure 5a) and edgewise direction (figure 5b) was plotted.

The flexible blade showed a significant increase in both the spanwise and edgewise deflections. The flapwise deflection should not be a problem unless the deformations are large enough to hit the tower in which failure would occur. The edgewise deflections indicate that the chamber of the blade has changed. This could lead to slight improvements in blade performance.

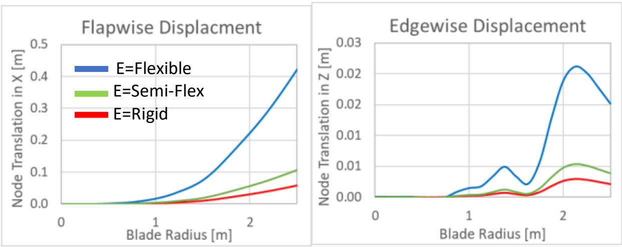

Fig. 5. (a=left) Flapwise & (b=right): Edgewise displacement along the blade radius under wind loading conditions

The twist angle or torsion of the blade did not seem to differ between the three blades, with a maximum percentage difference of 0.3% between the rigid and fully flexible blade occurring at the blade tip. This suggests that flexibility had no effect on altering the angle of attack.

Next, in order to check whether an increased chamber caused by the edgewise deflections improves the performance, the power coefficient, Cp, was plotted against the tips speed ratio, TSR, for an average turbulent wind speed of 7.5 m/s in Figure 6. The performance curve for each of the blades is almost identical despite the large difference in deflections. The difference was around one tenth of a percent. This result from the QBlade simulations indicates that a flexible blade made from more sustainable materials could produce comparable power to its fibreglass counterparts.

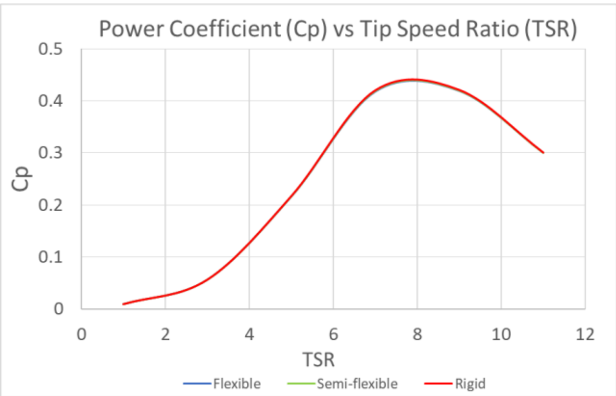

Fig. 6. Performance curve comparing the flexible, semi-flexible and rigid blades.

However, there needs to be an element of caution with these results as it could point to potential limitations with the BEM theory. It was predicted that the performance of the highly flexible blade would sway significantly to either a high or low Cp.

C. Effects of Flexibility on Fatigue Life

The rainflow counting algorithm in MATLAB analysed the cyclic stress profile (computed using Equation 4) and was used to assess the damage cycles of each stress amplitude/mean stress combination. Comparing the mean stress values of each blade, the rigid blade gave the highest mean stress value at 8 MPa, the semi-flexible blade showed a slight reduction at 7.8 MPa, and the flexible blade gave a significant reduction in the mean stress at 6.5 MPa.

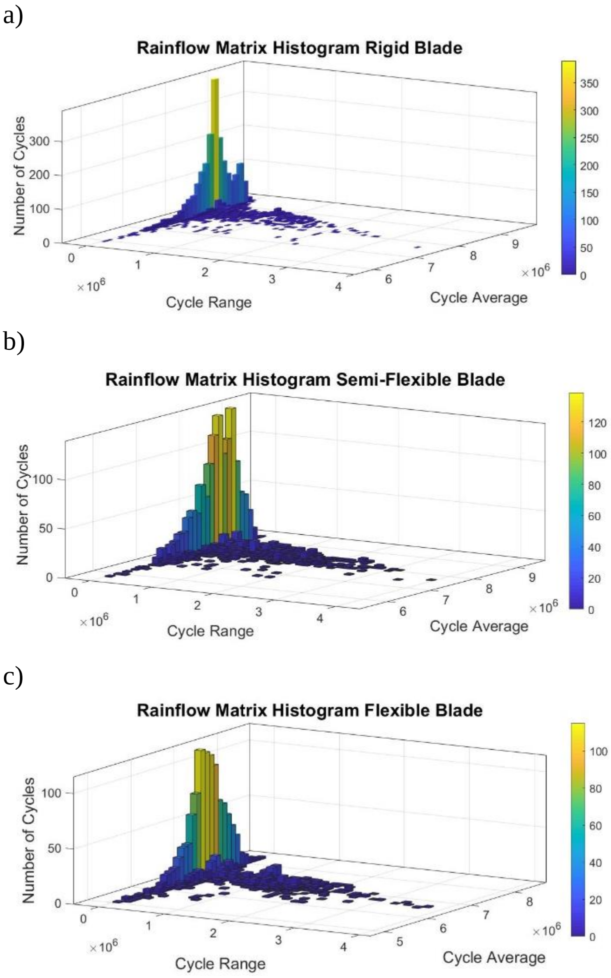

Fig. 7 gives the rainflow for the (a) rigid, (b) semi-flexible and (c) fully flexible blades, respectively.

The mean stress values in isolation cannot determine the fatigue damage and the frequency and amplitude of the stress waves must be accounted for.

The rigid blade in Figure 7a shows a high frequency (signified by the high spike of 300+ cycles) of very small amplitude waves. The small amplitude is likely not to cause any significant damage but might be an issue if occurs frequently. Figures 7b and 7c both show that increasing the flexibility of the blade causes a more distributed rainflow where the stress waves varies quite significantly in size over the simulated time period. Although the magnitude of the stress waves may be larger than the rigid blade they occur much less frequently.

The damage calculated for each individual cycle was summed to produce the cumulative damage, *D*, (Equation 5) to calculate the lifespan, shown in Figure 8. For the wind conditions of 7.5 m/s modelled in the initial simulation, the rigid blade gives a far superior lifespan. However, the lines in Figure 8 intersect at around 10 m/s. Due to the large gradient in the red line for the rigid blade, the fatigue life quickly drops by three orders of magnitude and the blade would fail at wind speeds above 11 m/s.

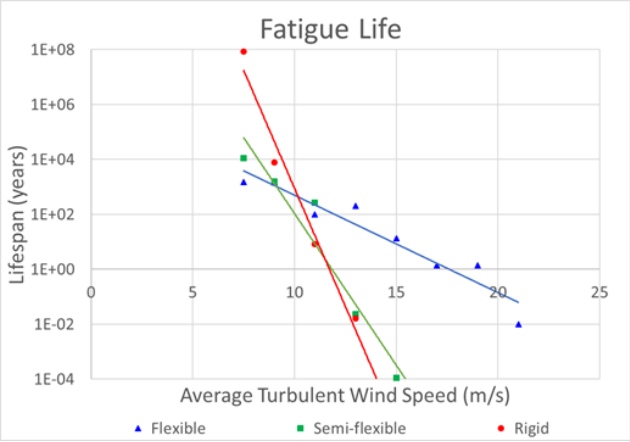

Fig. 8. Life span of the flexible, semi-flexible and rigid blades for a wind speeds ranging from 7.5 m/s to 21 m/s.

The green squares and line represent the semi-flexible blade which gives a slight reduction in the gradient, but it is the flexible blade, shown by the blue triangles and line, that strongly outperforms the other blades at high wind speeds. The results are clear that in areas which experience high winds, a flexible blade could be beneficial in reducing the blade loading and therefore increase the lifespan of the blade. The flexible blade managed to decrease the bending moment and stresses on the blade root, just like the plants were shown to bend to resist high wind forces. Alternatively, in regions that experience low winds on a regular basis, a more rigid blade would be a better choice.

This study correlated the life span of the blade directly from the moments and forces on the blade root only, since the blade design was the focus point. Maintenance issues and failures can come from a range of the mechanical and electrical components and a lifecycle analysis such as an FMEA requires an in-depth look at all components.

The fatigue life results proved to be highly sensitive to both the *m* parameter (S-N slope) and the compressive and tensile strength of the material in Equation 6. Material properties tables vary between sources and whilst care was taken upon selection of these properties, it must be noted that the final lifespan result are sensitive to their choice.

4. Discussion and Conclusion

While this research is preliminary, it highlights opportunities to improve the performance of turbines through the exploitation of design options which are easy to manufacture, even in parts of the world where manufacturing and maintenance facilities are limited. The corrugated aerofoils gave the advantage of delaying stall, with the corrugated skin proving a better option for adaptation to wind turbine blades because it had similar lift to drag characteristics to the smooth aerofoil. Flexible materials such as bamboo laminates are accessible even to remote areas where local alternatives can be sourced. Manufacturers face a problem in recycling fibreglass material at the end of life so flexible blades offers a sustainable solution that has been shown here to produce comparable performance and increased design lifetime.

This research has identified some promising underlying aerodynamic processes which hint at how a turbine rotor would passively adapt to the conditions. These two new concepts were tested individually, and once proof of concept is reviewed, higher computational effort is required to introduce the two ideas into one system and analyse using coupled fluid-structure interactions (FSI). Then the flexibility and corrugations can be combined and fully optimised for a small wind turbine system and validated with physical test turbine.

The challenge remains to identify surface features, material properties, and blade designs which respond favourable to the challenging aerodynamic conditions for small wind turbines.

Acknowledgements

This work was supported by the Institute of Mechanical, Process and Energy Engineering at Heriot-Watt University in Edinburgh. Additionally, the author would like to thank Dr Wolf Früh for his supervision and support.

References

[1] F. Fish, P. Weber, M. Murray, L. Howle, “The tubercles on humpback whales' flippers: application of bio-inspired technology”, Integr Comp Biol (2011), Vol. 51, pp. 203-13.
[2] E. d. Langre, “Effects of Wind on Plants”, Annual Review of Fluid Mechanics (2008). Vol. 40, pp. 141-168.
[3] T. Q. Le et al, “Improvement of the aerodynamic performance by wing flexibility and elytra–hind wing interaction of a beetle during forward flight”, Journal of The Royal Society Interface (2013). Vol. 10,
[4] X. Lachenal, S. Daynes and P.M. Weaver, “Review of morphing concepts and materials for wind turbine blade applications”, Wind Energy (2013). Vol. 16, pp. 283 – 307.
[5] S.P. Evans, D.R Bradney and P.D. Clausen, “Aeroelastic measurements and simulations of a small wind turbine operating in the built environment”, Journal of Physics: Conf. Ser. (2016), Vol. 753.
[6] D.W. McPhee and A. Bayene, “Fluid-structure interaction analysis of a morphing vertical axis wind turbine”, Journal of Fluids and Structures (2016), Vol. 60, pp. 143 – 159.
[7] J. Piquee et al, “Aerodynamic analysis of a generic wing featuring an elasto-flexible lifting surface”, Adv. Aerodyn (2019). Vol. 1, p. 20.
[8] V. Cognet, S. Courrech du Pont, I. Dobrev, F. Massouh and B. Thiria, “Bioinspired turbine blades offer new perspectives for wind energy”, Proc. R. Soc. (2017). Vol. 473.
[9] D. Manshadi, “Numerical evaluation of passive control of shock wave/boundary layer interaction on NACA0012 airfoil using jagged wall”, Acta Mechanica Sinica (2016). Vol. 32, pp. 792-804.
[10] Y. Xia, O. Bilgen, M. Friswell “The effect of corrugated skins on aerodynamic performance”, Journal of Intelligent Material Systems and Structures (2014). Vol. 25, pp. 786-794.
[11] D. Marten, “QBlade Guidelines v 0.6”, TU , Berlin, 2012.
[12] M. O. L. Hansen, Aerodynamics of Wind Turbines: second edition, Earthscan, (2008).
[13] J.M Jonkman, M.L. Buhl, “FAST users guide”, National Renewable Energy Laboratory, (2005).
[14] Germanischer Lloyd, Guidelines for the certification of wind turbines, Germanischer Lloyd, Hamburg (2010), pp. 197-204.